Acta Materia Medica

Research Article

Smart stimuli-responsive carrier-free nanoassembly of SN38 prodrug as efficient chemotherapeutic nanomedicine

Graphical abstract

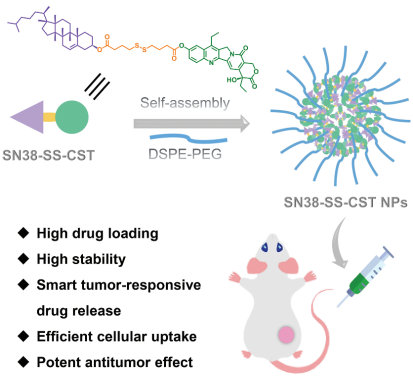

Highlights

- A novel SN38 prodrug that self-assembles into prodrug nanoassemblies independently of carrier materials is reported.
- SN38 prodrug nanoassemblies specifically release active SN38 in response to the redox environment inside tumor tissues but remain intact in other normal tissues.
- The smart stimuli-responsive SN38 prodrug nanoassemblies elicited significantly better antitumor outcomes than commercial Campto®.

Authors

Guanting Li, Qianhui Jin, Fengli Xia, Shuwen Fu, Xuanbo Zhang, Hongying Xiao, Chutong Tian, Qingzhi Lv, Jin Sun, Zhonggui He and Bingjun Sun

Correspondence

hezhgui_student@aliyun.com (Z. He); sunbingjun_spy@sina.com (B. Sun)

In brief

A smart stimuli-responsive SN38 prodrug nanoassembly for efficient cancer therapy is reported. SN38 prodrug nanoassemblies provide multiple therapeutic advances including ultrahigh drug loading, good colloidal stability, tumor-specific drug release, and high cellular uptake, thereby potently inhibiting colon cancer growth without causing systemic toxicity.

https://doi.org/10.15212/AMM-2023-0003

Acta Materia Medica

Research Article

Smart stimuli-responsive carrier-free nanoassembly of SN38 prodrug as efficient chemotherapeutic nanomedicine

Guanting Li[a], Qianhui Jin[a], Fengli Xia[a], Shuwen Fu[b], Xuanbo Zhang[a], Hongying Xiao[a], Chutong Tian[a], Qingzhi Lv[c], Jin Sun[a], Zhonggui He[a,*] and Bingjun Sun[a,*]

[a]Department of Pharmaceutics, Wuya College of Innovation, Shenyang Pharmaceutical University, Shenyang 110016, P. R. China
[b]School of Pharmacy, Shenyang Pharmaceutical University, Shenyang 110016, P. R. China
[c]School of Pharmacy, Binzhou Medical University, Yantai 264000, P. R. China

***Correspondence:** hezhgui_student@aliyun.com (Z. He); sunbingjun_spy@sina.com (B. Sun)

Received: 18 January 2023; Revised: 9 February 2023; Accepted: 10 February 2023

Published online: 24 February 2023

DOI 10.15212/AMM-2023-0003

ABSTRACT

The compound 7-ethyl-10-hydroxy-camptothecin (SN38) is a broad-spectrum antitumor agent whose applications are greatly limited by its poor solubility. Therefore, irinotecan, the hydrophilic derived prodrug of SN38, has been developed as the commercial formulation Campto® for colorectal cancer. However, only 1% to 0.1% of irinotecan is converted to active SN38 in vivo, thus leading to unsatisfactory antitumor activity in clinical settings. Herein, we report a smart stimuli-responsive SN38 prodrug nanoassembly for efficient cancer therapy. First, SN38 was conjugated with an endogenous lipid, cholesterol (CST), via a redox dual-responsive disulfide bond (namely SN38-SS-CST). The prodrug self-assembled into uniform prodrug nanoassemblies with good colloidal stability and ultrahigh drug loading. SN38-SS-CST NPs released sufficient SN38 in the redox environments of tumor cells but remained intact in normal tissues. Finally, SN38-SS-CST NPs potently inhibited the growth of colon cancer without causing systemic toxicity, thus indicating their promise as a translational chemotherapeutic nanomedicine.

Keywords: Prodrug nanoassembly, SN38, Redox responsiveness, Nanomedicine, cancer therapy

1. INTRODUCTION

Chemotherapy has long been the first-line choice for cancer treatment [1]. Among the various cytotoxic chemo-drugs, 7-ethyl-10-hydroxy-camptothecin (SN38), a semi-synthetic camptothecin derivative, has broad and potent antitumor efficacy by inhibiting the activity of topoisomerase I, thereby causing lethal DNA damage [2]. However, the extreme hydrophobicity and poor solubility of SN38 have severely limited its applications. Although the carboxylic acid ester form of SN38 improves its solubility, its systemic toxicity is also increased [3, 4]. The water-soluble derivative of SN38 irinotecan (Campto®) was developed and approved by the FDA for the treatment of colorectal cancer [5]. Irinotecan is synthesized by conjugation of SN38 with a 4-piperidinopiperidine group via an easter bond. To exert cytotoxicity, irinotecan must be converted to active SN38 through cleavage of the easter bond. Unfortunately, the hydrolysis of the easter bond is so inefficient in vivo that only 1% to 0.1% of irinotecan is metabolized into SN38, thereby greatly diminishing the antitumor activity of irinotecan [6]. Consequently, the cytotoxicity of irinotecan is 100 to 1,000-fold lower than that of SN38 [7].

Nanoparticulate drug delivery systems (Nano-DDSs) have been among the most successful facilitators of chemotherapy [8-11]. Well-designed Nano-DDSs protect loaded drugs from premature metabolism and clearance, and increase tumor accumulation through the known enhanced permeability and retention effect [12, 13]. Conventional nano-DDSs (e.g., liposomes and microspheres) are usually used to encapsulate drugs through intermolecular nonvalent interactions, such as hydrophobic interactions and electrostatic interactions between the carrier material and drug [14, 15]. However, SN38 has an extremely flat and highly rigid structure with a high crystallization tendency [16]. Therefore, SN38 has very low affinity toward carrier materials, thus resulting in low drug loading efficiency, poor stability and premature drug leakage. In addition, overused carrier

materials may introduce carrier-associated allergy and toxicity [17]. The rational design of SN38-based nanomedicines remains a challenge.

Recently, prodrug nanoassemblies have emerged as a versatile nanoplatform for antitumor drug delivery [18]. Through a simple one-step nanoprecipitation method, prodrug molecules self-assemble into nanosized assemblies independently of carrier materials [19]. Prodrug nanoassemblies act as both the carrier and cargo, and have shown ultrahigh drug loading (>30%) and negligible carrier-associated adverse effects [18]. Additionally, the simple fabrication helps overcome barriers to industrial translation. More importantly, according to the characteristics of the tumor microenvironment (TME), smart tumor stimulus-responsive prodrugs have been widely developed to facilitate tumor-specific drug release [20, 21]. By combining the merits of both techniques, stimulus-responsive prodrug nanoassemblies provide a potent and safe antitumor platform.

Herein, we report smart stimuli-responsive SN38 prodrug nanoassemblies for efficient cancer therapy. SN38 was conjugated with the endogenous lipid cholesterol (CST) via a redox dual-responsive disulfide bond (termed SN38-SS-CST). Through a one-step nanoprecipitation method, SN38-SS-CST self-assembled into nanoassemblies (SN38-SS-CST NPs) of approximately 100 nm, driven by hydrophobic interactions, π-π stacking and hydrogen bonding. In the redox-overexpressed TME, SN38-SS-CST NPs released sufficient SN38 and showed no burst release under normal physiological conditions. Finally, SN38-SS-CST NPs potently inhibited the growth of colon cancer without causing systemic toxicity, thus indicating their potential as a translational nanomedicine for chemotherapy.

2. RESULTS AND DISCUSSION

2.1 Chemical synthesis

To construct a self-assembling prodrug, we chose CST as the side chain to conjugate with SN38 (**Figure S1**). In addition, because the disulfide bond has been reported to be a redox dual-responsive chemical bond that facilitates tumor-specific drug release [22], we developed a disulfide-bridged SN38-SS-CST prodrug. According to ^{1}H nuclear magnetic resonance spectroscopy (NMR) and mass spectrometry, intermediate CST-SS-COOH and SN38-SS-CST were successfully synthesized (**Figure S2–5**). The purity of SN38-SS-CST reached 99.74% (**Figure S6**).

2.2 Characterization of prodrug nanoassemblies

As shown in **Figure 1a**, SN38-SS-CST self-assembled into prodrug nanoassemblies through the one step nanoprecipitation method, independently of the carrier material. Only a small amount of DSPE-PEG$_{2k}$ (20%, w/w) was added to decrease the free surface energy and increase stability. The self-assembled SN38-SS-CST NPs were spherical particles of approximately 100 nm (**Figure 1b,c** and **Table S1**), and showed an ultrahigh drug loading of 31.94%. After laser irradiation, SN38-SS-CST NPs showed a clear Tyndall effect, thus indicating colloidal properties. In addition, the negative zeta protentional (–22.3 mV) helped maintain the colloidal stability of the prodrug nanoassemblies.

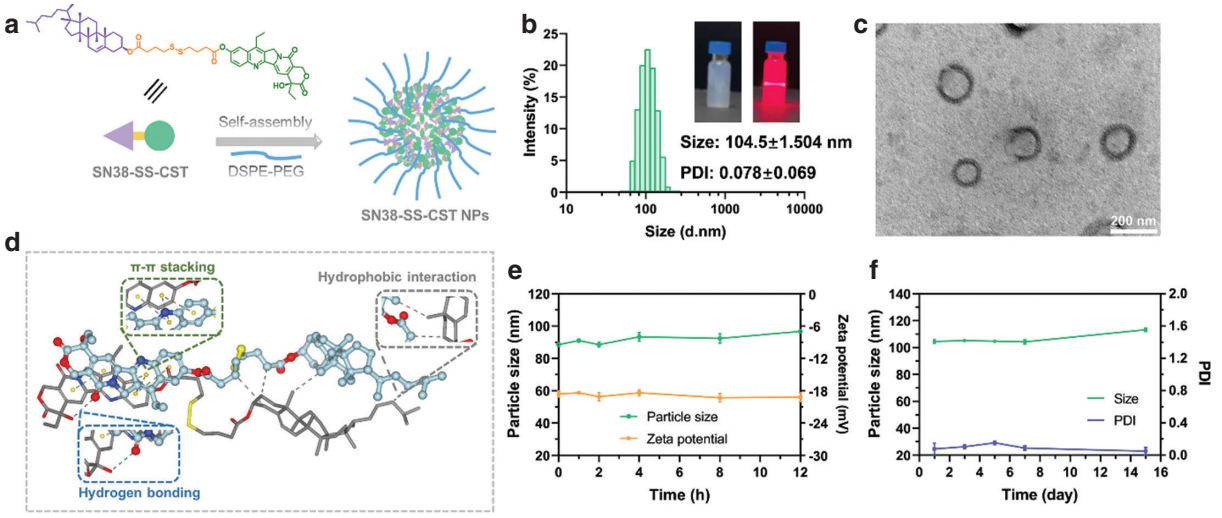

Figure 1 | Characterization of prodrug nanoassemblies.
a) Schematic illustration of the self-assembly of SN38-SS-CST NPs. b) Size distribution and images of SN38-SS-CST NPs. c) Transmission electron microscopy image of SN38-SS-CST NPs. Scale bar = 200 nm. d) Molecular dynamics simulations of the self-assembly of SN38-SS-CST NPs. Green lines indicate π-π stacking. Blue lines indicate hydrogen bonding. Gray lines indicate hydrophobic interactions. e) Colloidal stability of SN38-SS-CST NPs in PBS (pH 7.4) containing 10% FBS. f) Storage stability of SN38-SS-CST NPs at 4°C.

Acta Materia Medica

2.3 Self-assembly mechanisms

The self-assembly process of SN38-SS-CST NPs was analyzed with molecular dynamics simulations. The conformation of the prodrug molecules (**Figure 1d**) revealed that during the self-assembly process, the aromatic rings of S38 molecules were packed through π-π stacking interactions, and the CST molecules clustered through hydrophobic interactions. In addition, the hydroxyl groups of SN38 participated in hydrogen bonding. The diameters according to molecular dynamics simulation also verified the spontaneous self-assembly of SN38-SS-CST (negative grid score and positive internal energy repulsion) and indicated that the process was driven primarily by Van der Waals forces (**Table S2**).

2.4 Colloidal stability

First, we investigated the storage stability of SN38-SS-CST NPs at 4°C. During a 15-day storage period, no clear changes in particle size were observed, thus indicating that SN38-SS-CST NPs can be stored for long time periods for future use (**Figure 1f**). In addition, to stimulate in vivo conditions, we incubated SN38-SS-CST NPs with PBS (pH 7.4) containing 10% fetal bovine serum (FBS). As shown in **Figure 1e**, the SN38-SS-CST NPs remained stable and showed almost no changes in particle size and zeta potential during the 12 h incubation. Thus, SN38-SS-CST NPs have superior in vitro and in vivo colloidal stability.

2.5 In vitro drug release

Prodrugs ideally release active parent drugs at targeted sites but remain intact in other cells and tissues [23]. Both oxidative reactive oxygen species (ROS) and reductive glutathione (GSH) are present in the TME [24]. Consequently, various tumor-specific stimuli responsive chemical bonds have been developed to produce smart antitumor prodrugs and nanomedicines [25, 26]. Among them, disulfide bonds have been reported to have redox dual-responsiveness [27, 28]. Therefore, we introduced a disulfide bond into the SN38-SS-CST prodrug. On the basis of previous research [27], the release mechanisms are illustrated in **Figure 2a**.

The stimulus-responsive drug release profiles of SN38-SS-CST NPs were investigated by using H_2O_2 as a ROS stimulus and DTT as a GSH stimulus. As depicted in **Figure 2b,c**, the stimulus-dependent release of SN38 was dependent on time and concentration. SN38-SSCST NPs showed much better reductive responsiveness than oxidative responsiveness. Approximately 60% of SN38 was released in the presence of 10 mM DTT in 24 h. Notably, no burst release of SN38 was observed in the absence of stimuli, thus demonstrating excellent selectivity of SN38-SS-CST NPs toward redox-overexpressed tumor cells and normal cells.

2.6 Cytotoxicity

The cytotoxicity of SN38-SS-CST NPs and Campto was compared in CT26 and 4T1 cells. As shown in **Figure 3a,b**

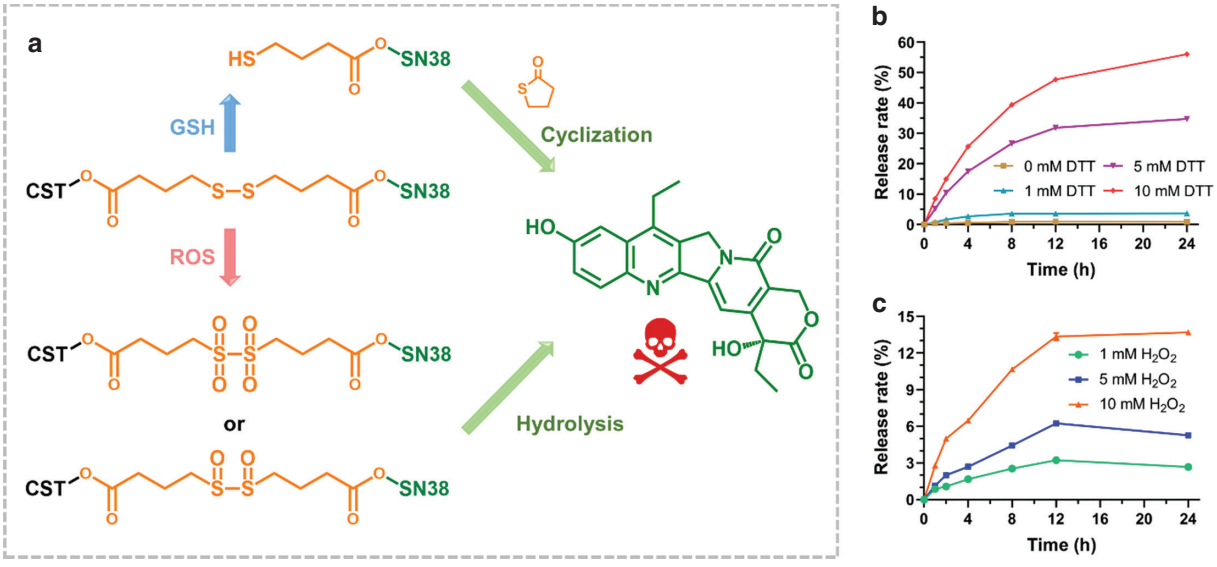

Figure 2 | In vitro redox-responsive drug release.
a) Proposed release mechanisms of SN38-SS-CST NPs. In GSH medium, the SN38-sulfhydryl compound (SN38-SH) is first released through sulfur exchange between SN38-SS-CST and GSH. The exposed sulfhydryl of SN38-SH attacks the adjacent ester bond in intramolecular cyclization, and SN38 is released. In ROS medium, the disulfide is oxidized into hydrophilic sulfoxide or sulfone, thereby facilitating hydrolysis of the adjacent ester bond and SN38 release. b) GSH stimulus-responsive release profiles of SN38-SS-CST NPs. c) ROS stimulus-responsive release profiles of SN38-SS-CST NPs. Data are presented as means ± SD (n = 3).

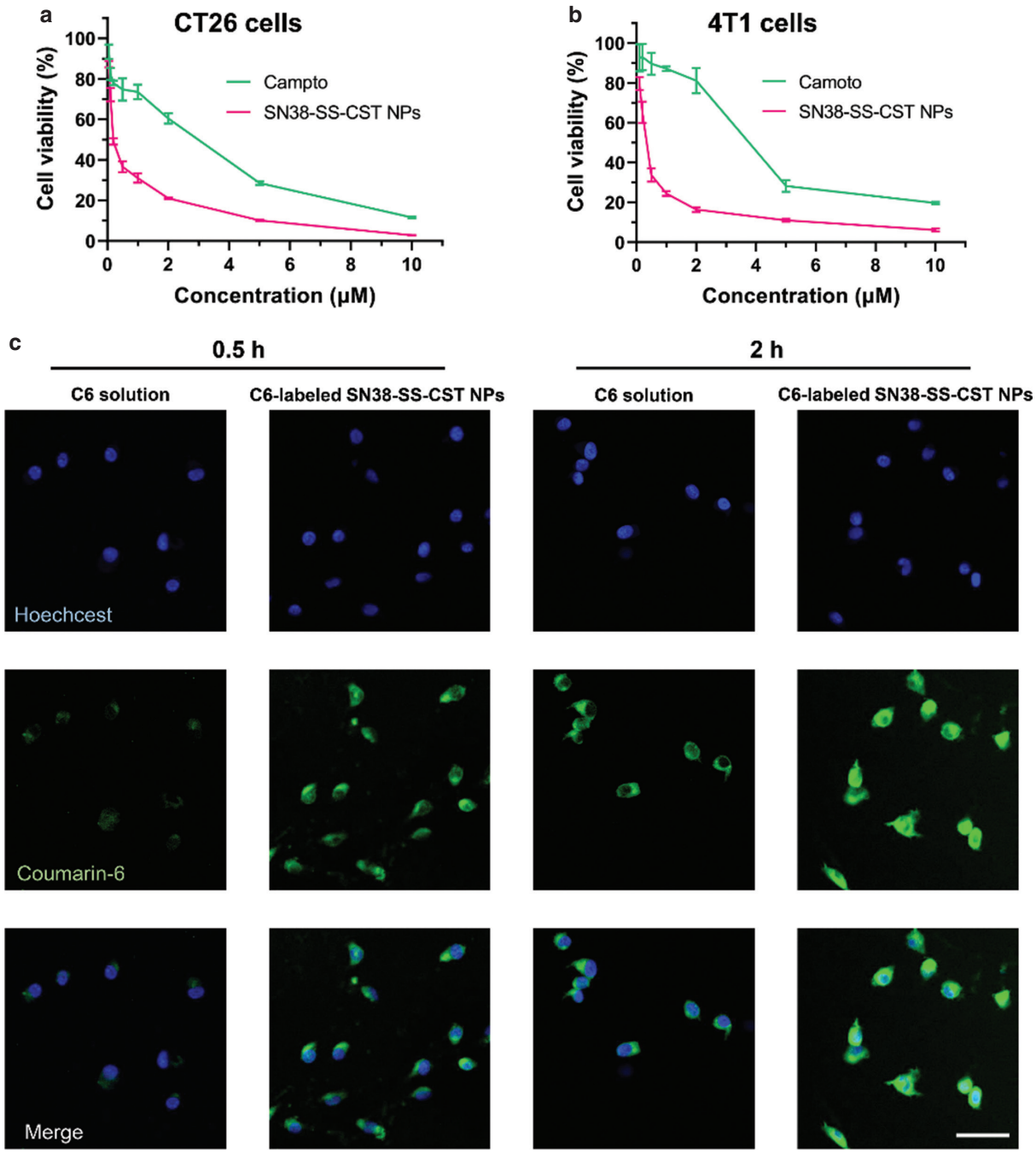

Figure 3 | Cytotoxicity and cellular uptake.
a) Viability of CT26 cells treated with the formulations. b) Viability of 4T1 cells treated with the formulations. Data are presented as means ± SD (n = 3). c) CLSM images of CT26 cells incubated with free C-6 or C-6-labeled SN38-SS-CST NPs for 0.5 h and 2 h. Scale bar = 50 μm.

and **Table S3**, the half-maximal inhibitory concentration (IC_{50}) of Campto (2,063 nM on CT26 cells; 2,638 nM on 4T1 cells) was much higher than that of SN38-SS-CST NPs (291.2 nM on CT26 cells; 335.7 nM on 4T1 cells). The poor cytotoxicity of Campto was attributed to the slow hydrolysis rate of the easter bond of irinotecan, thus leading to slow and inefficient release of active SN38. In contrast, SN38-SS-CST NPs rapidly released sufficient SN38 in tumor cells, thereby achieving potent cytotoxicity.

2.7 Cellular uptake

The cellular uptake efficiency of prodrug nanoassemblies was investigated on CT26 cells. Free coumarin-6 (C-6) solution and C-6-labeled SN38-SS-CST NPs were incubated with CT26 cells for 0.5 h or 2 h. Subsequently, the intracellular fluorescence intensity was evaluated with confocal laser scanning microscopy (CLSM). As displayed in Figure 3c, the intracellular fluorescence intensity of C-6-labeled SN38-SS-CST NPs was much higher than that of free C-6 solution at both time intervals. These results indicated that prodrug nanoassemblies are sufficiently endocytosed by tumor cells.

2.8 In vivo antitumor effects

The in vivo antitumor efficacy of SN38-SS-CST NPs was investigated on xenograft CT26 bearing BALB/c mice. The formulations were administered to the mice every other day in a total of five injections (Figure 4a). As shown in Figure 4b,d,e, CT26 tumors rapidly grew in an unrestricted manner the PBS-treated group. Commercial Campto moderately inhibited tumor growth, yet the tumor volume reached approximately 800 mm^3 by the end of treatment. In comparation, SN38-SS-CST NPs showed potent tumor inhibitory effects in terms of both tumor volume and tumor burden. The H&E staining of tumors

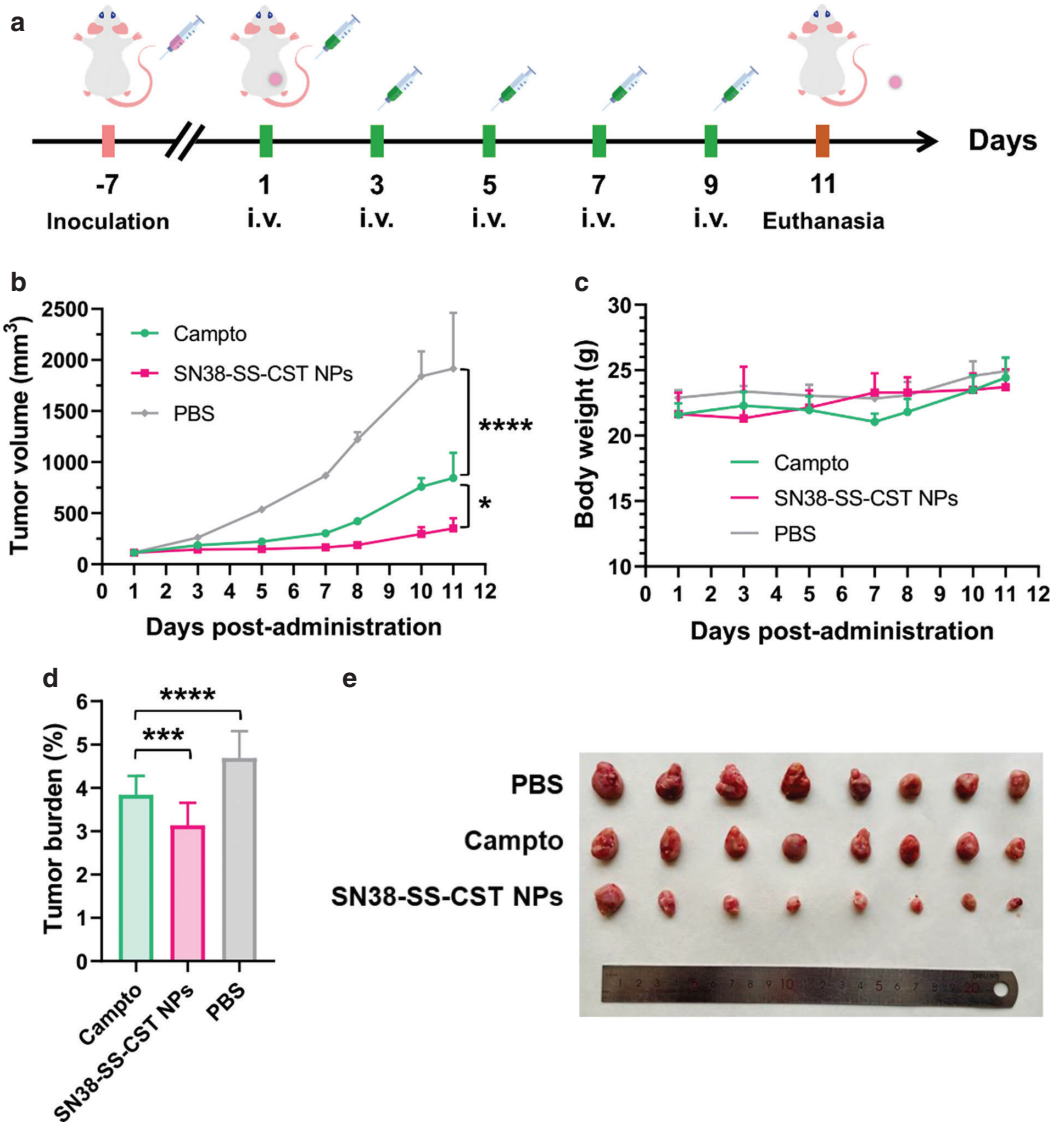

Figure 4 | In vivo antitumor efficacy.

a) Pharmacodynamics study protocol. b) Tumor volumes of CT26 bearing mice during the treatment. c) Body-weight changes in CT26 bearing mice during treatment. d) Tumor burden of CT26 bearing mice at the end of treatment. e) Images of resected CT26 tumors at the end of treatment. Data are presented as means ± SD (n = 8), *$p < 0.05$, ***$p < 0.001$, ****$p < 0.0001$.

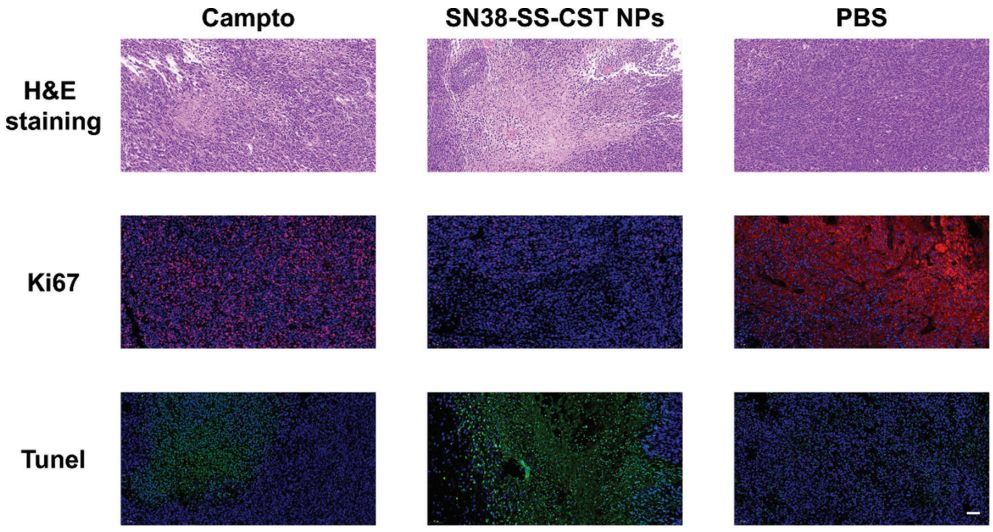

Figure 5 | H&E staining, Ki67 immunofluorescence and TUNEL staining of resected CT26 tumors. Scale bar = 50 μm.

revealed that the SN38-SS-CST NP-treated group had more necrotic areas than the control (Figure 5). In addition, immunofluorescence indicated that SN38-SS-CST NPs successfully inhibited tumor proliferation (Ki67) and induced more tumor apoptosis than the control (TUNEL).

Systemic toxicity was evaluated on the basis of body weight, hepatorenal function and H&E staining of major organs. Neither formulation led to body-weight changes, hepatorenal damage or discernible histological lesions in major organs (Figure 4c and Figure S7–8), thus indicating the excellent safety of SN38-SS-CST NPs. Overall, SN38-SS-CST NPs overcame the drawbacks of commercially formulated Campto, thus providing a safe and potent antitumor platform with translational potential.

3. CONCLUSION

In this work, we developed a tumor redox-responsive carrier-free nanoplatform for the efficient delivery of SN38. First, the endogenous lipid CST was conjugated with SN38 via a disulfide bond to form the SN38-SS-CST prodrug. Through a simple one-step nanoprecipitation method, SN38-SS-CST self-assembled in uniform nanoassemblies of approximately 100 nm with good colloidal stability. Under redox environments, SN38-SS-CST NPs rapidly released active SN38 yet showed no burst release under normal physiological conditions. Finally, the SN38-SS-CST NPs demonstrated potent antitumor efficacy in both cell studies and in vivo studies, without causing additional toxic effects. Therefore, SN38-SS-CST NPs overcome the drawbacks of commercial Campto and may have value in translational applications.

4. MATERIALS AND METHODS

4.1 Materials

SN38 and 3-(4,5-dimethylthiazol-2-yl)-2,5-diphenyl tetrazolium bromide (MTT) were purchased from Dalian Meilun Biotechnology Co., Ltd; CST, 4,4′-dithiodibutyric acid and 4-dimethylaminopyridine were purchased from Macklin Co., Ltd.; 1-ethyl-3(3-dimethylpropylamine) carbodiimide and 1-hydroxybenzotriazole were purchased from Aladdin Co., Ltd.; and 1,2-distearoylsn–glycero-3-phosphoethanolamine-N-methyl (polyethylene glycol)-2000 (DSPE-PEG_{2k}) was obtained from Shanghai Advanced Vehicle Technology Pharmaceutical Ltd. (Shanghai, China). Other reagents in this study were of analytical grade.

4.2 Chemical synthesis

The chemical synthesis of the SN38-SS-CST prodrug is shown in Figure S1. First, 4,4′-dithiodibutyric acid (0.5 mmol) and acetic anhydride (5 mL) were mixed and stirred at room temperature for 4 h. Subsequently, acetic anhydride was removed through rotary evaporation to obtain 4,4′-dithiodibutyric anhydride. Afterward, 4,4′-dithiodibutyric anhydride, 4-dimethylaminopyridine (0.15 mmol) and CST (0.6 mmol) were dissolved in anhydrous dichloromethane. The reaction proceeded at room temperature for 12 h under stirring. The completion of the reaction was monitored with thin-layer chromatography. Finally, the product was extracted and separated by column chromatography (with dichloromethane-methanol as the mobile phase). The product (CST-SS-COOH) was a white solid (yield 73%). The chemical structure of CST-SS-COOH was identified with NMR.

Subsequently, SN38 (0.3 mmol), 1-ethyl-3(3-dimethylpropylamine) carbodiimide (0.4 mmol), 4-dimethylaminopyridine (0.1 mmol), 1-hydroxybenzotriazole (0.3 mmol) and CST-SS-COOH (0.3 mmol) were dissolved in anhydrous dichloromethane. The reaction proceeded at in room temperature for 12 h under stirring. After completion of the reaction, the product was extracted and separated by preparative liquid chromatography (with acetonitrile as the mobile phase). The product (SN38-SS-CST) was yellow solid (yield 56%). The chemical structure of SN38-SS-CST was identified with mass spectrometry and NMR. The purity of SN38-SS-CST was assessed with high performance liquid chromatography at a wavelength of 365 nm.

4.3 Preparation and characterization of prodrug nanoassemblies

Prodrug nanoassemblies of SN38-SS-CST were prepared through the typical one step nano-precipitation method. In brief, SN38-SS-CST (2 mg) was dissolved in 300 μL of acetone, and DSPE-PEG_{2k} (0.5 mg, 20% w/w) was dissolved in 100 μL of ethanol. The drug-containing solution was then mixed and added dropwise to 2 ml of aqueous solution under vigorous stirring for 10 min. The organic solvent was removed through rotary evaporation to obtain SN38-SS-CST NPs. The dye-labeled prodrug nanoassemblies were prepared through the same procedure with the addition of coumarin-6 (C-6) into the drug-containing solution. The particle size and zeta potential of SN38-SS-CST NPs were assessed with a Zetasizer instrument. The morphology of SN38-SS-CST NPs was observed with a transmission electron microscope. The sample for observation were stained with 2% phosphotungstic acid.

4.4 Self-assembly mechanisms

The self-assembly mechanisms of SN38-SS-CST NPs were investigated with molecular dynamics simulations. First, the three-dimensional conformation of SN38-SS-CST was assessed with Sybyl software. Subsequently, the self-assembly process of SN38-SS-CST NPs was analyzed in Discovery Studio 2017 Visualizer software. The simulated box center parameter was (-6.049, 0.406, 0.869). The simulated box size parameter was (48.897, 40.062, 39.957). The maximum output conformation number was 9.

4.5 Colloidal stability of prodrug nanoassemblies

To investigate the storage stability of SN38-SS-CST NPs, we incubated the samples at 4°C for 15 days. The particle sizes of prodrug nanoassemblies were measured on days 0, 3, 5, 7 and 15. To investigate the colloidal stability of SN38-SS-CST NPs under biological conditions, we incubated and SN38-SS-CST NPs in PBS containing 10% FBS (pH 7.4) at 37°C under shaking. The samples were collected, and the particle size and zeta potential were measured at 0, 1, 2, 4, 8 and 12 h.

4.6 In vitro drug release

To investigate the stimulus responsiveness of SN38-SS-CST NPs, we used a medium comprising PBS-ethanol solution (80: 20, v/v) with or without H_2O_2 or DTT as stimuli (1, 5 or 10 mM). Briefly, SN38-SS-CST NPs (200 μg/mL, SN38 equivalent) were placed in the release medium at 37°C under shaking. At selected time intervals (1, 2, 4, 8, 12 and 24 h), samples were collected (n = 3 per group). The concentration of released SN38 was determined with high performance liquid chromatography at a wavelength of 365 nm.

4.7 Cell culture

CT26 colon tumor cells were purchased from Dalian Meilun Biotechnology Co., Ltd (Dalian, China), and 4T1 breast tumor cells were purchased from COBIOER Biotechnology Co., Ltd. (Nanjing, China). The cells were cultured in Gibco RPMI 1640 medium containing 10% FBS, streptomycin (100 μg/mL) and penicillin (100 units/mL). The cells were grown in a cell incubator at 37°C under a 5% CO_2 atmosphere.

4.8 Cytotoxicity

The cytotoxicity of SN38-SS-CST NPs and Campto was investigated in CT26 and 4T1 cells with MTT assays. The cells were pre-seeded into 96-well plates (3,000 cells per well) and incubated for 24 h before treatment. Subsequently, the medium was discarded and replaced with medium containing different drug concentrations. After incubation for another 48 h, the drug-containing medium was discarded, and 25 μL MTT solution (5 mg/mL) was added to each well and incubated for 4 h. Finally, MTT solution was discarded, and 200 μL of DMSO was added to each well. After shaking, the absorbance at 570 nm was detected with a microplate reader. The IC_{50} values were calculated in GraphPad prism 8.0 software.

4.9 Cellular uptake

The cellular uptake efficiency of prodrug nanoassemblies was investigated in CT26 cells with C-6-labeled SN38-SS-CST NPs and C-6 solution. First, CT26 cells were seeded in 24-well plates (5×10^4 cells per well) and incubated for 24 h before treatment. Subsequently, the medium was discarded and replaced with C-6-labeled SN38-SS-CST NPs or C-6 solution (250 ng/ml, C-6 equivalent). After incubation for 0.5 h or 4 h, cells were washed with cold PBS three times, and 4% formaldehyde was used to fix the cells. After further washing, Hoechst was used to counterstain the nuclei. The prepared coverslips were observed with CLSM.

4.10 Animal studies

The animal studies were performed under the guidance and supervision of the Institutional Animal Ethical Care Committee of Shenyang Pharmaceutical University.

4.11 In vivo antitumor efficacy

The antitumor efficacy of SN38-SS-CST NPs and Campto was investigated on xenografted CT26 tumor models. For construction of the CT26 tumor models, CT26 cells (5×10^6 cells per 100 μL) were subcutaneously injected into the flanks of male BALB/c mice. When the tumor volume reached approximately 100 mm^3, the treatments started. SN38-SS-CST NPs and Campto were administered to the mice every other day (3 mg/kg, SN38 equivalent) in a total of five injections (n = 8 for each group). Tumor volume and body weight were monitored during the treatment. At 2 days after the last treatment, the mice were scarified. Blood samples were collected, and major organs including the heart, liver, spleen, lungs and kidneys, as well as tumors were collected. The tumors were weighed. Hepatorenal function, H&E staining and immunofluorescence staining were conducted by Servicebio Co., Ltd (Wuhan, China). The tumor volume was calculated as (long diameter × short diameter × 2)/2. The tumor burden was calculated as tumor weight/mouse weight.

4.12 Statistical analysis

All data are presented as mean ± SD. For statistical analysis, one-way analysis of variance and Student's t-test (two-tailed) were performed in GraphPad Prism 8.0 software. The thresholds for statistical differences were *$p < 0.05$, **$p < 0.005$, ***$p < 0.001$ and ****$p < 0.0001$.

ACKNOWLEDGEMENTS

This work was supported by the National Natural Science Foundation of China (no. 82272151, 82204318 and 82173766), Doctoral Scientific Research Staring Foundation of Liaoning Province (no. 2021-BS-130), General Program of Department of Education of Liaoning Province (no. LJKZ0953) and Shenyang Young and Middle-aged Science and Technology Innovation Talent Support Program (no. RC220389).

CONFLICTS OF INTEREST

The authors declare no conflicts of interest.

REFERENCES

[1] Bocci G, Kerbel RS: Pharmacokinetics of Metronomic Chemotherapy: A Neglected But Crucial Aspect. *Nature Reviews Clinical Oncology* 2016, 13:659–673.

[2] Voigt W, Matsui S, Yin MB, Burhans WC, Rustum YM: Topoisomerase-I Inhibitor SN-38 can Induce DNA Damage and Chromosomal Aberrations Independent from DNA Synthesis. *Anticancer Research* 1998, 18:3499–3505.

[3] Laizure SC, Herring V, Hu Z, Witbrodt K, Parker RB: The Role of Human Carboxylesterases in Drug Metabolism: Have We Overlooked Their Importance? *Pharmacotherapy* 2013, 33:210–222.

[4] Crawford J, Dale DC, Lyman GH: Chemotherapy-Induced Neutropenia: Risks, Consequences, and New Directions for its Management. *Cancer* 2004, 100:228–237.

[5] Sugiyama Y, Kato Y, Chu XY: Multiplicity of Biliary Excretion Mechanisms for the Camptothecin Derivative Irinotecan (CPT-11), its Metabolite SN-38, and its Glucuronide: Role of Canalicular Multispecific Organic Anion Transporter and P-Glycoprotein. *Cancer Chemotherapy & Pharmacology* 1998, 42 suppl:S44–S49.

[6] Yang W, Yang Z, Liu J, Liu D, Wang Y: Development of a Method to Quantify Total and Free Irinotecan and 7-ethyl-10-hydroxycamptothecin (SN-38) for Pharmacokinetic and Bio-Distribution Studies after Administration of Irinotecan Liposomal Formulation. *Asian Journal of Pharmaceutical Sciences* 2019, 14:687–697.

[7] Slatter JG, Su P, Sams JP, Schaaf LJ, Wienkers LC: Bioactivation of the Anticancer Agent CPT-11 to SN-38 by Human Hepatic Microsomal Carboxylesterases and the In Vitro Assessment of Potential Drug Interactions. *Drug Metabolism and Disposition* 1997, 25:1157–1164.

[8] Jong W: Drug delivery and Nanoparticles: Applications and Hazards. *International Journal of Nanomedicine* 2008, 3:133–149.

[9] Couvreur P: Nanoparticles in Drug Delivery: Past, Present and Future. *Advanced drug Delivery Reviews* 2012, 65:21–23.

[10] Zheng Y, Cao T, Han X, Cao P, Zhan Q: Structurally Diverse Polydopamine-Based Nanomedicines for Cancer Therapy. *Acta Materia Medica* 2022, 1:427–444.

[11] Zhou S, Shang Q, Wang N, Li Q, Song A, Luan Y: Rational Design of a Minimalist Nanoplatform to Maximize Immunotherapeutic Efficacy: Four Birds with One Stone. *Journal of Controlled Release* 2020, 328:617–630.

[12] Sun Q, Zhou Z, Qiu N, Shen Y: Rational Design of Cancer Nanomedicine: Nanoproperty Integration and Synchronization. *Advanced Materials* 2017, 29:1606628.

[13] Fu M, Han X, Chen B, Guo L, Zhong L, Hu P, et al.: Cancer Treatment: From Traditional Chinese Herbal Medicine to the Liposome Delivery System. *Acta Materia Medica* 2022, 1:486–506.

[14] Fu S, Li G, Zang W, Zhou X, Shi K, Zhai Y: Pure Drug Nano-Assemblies: A Facile Carrier-Free Nanoplatform for Efficient Cancer Therapy. *Acta Pharmaceutica Sinica B* 2022, 12:92–106.

[15] Li Y, Li L, Jin Q, Liu T, Sun J, Wang Y, et al.: Impact of the Amount of PEG on Prodrug Nanoassemblies for Efficient Cancer Therapy. *Asian Journal of Pharmaceutical Sciences* 2022, 17:241–252.

[16] Li Y, Kang T, Wu Y, Chen Y, Zhu J, Gou M: Carbonate Esters Turn Camptothecin-unsaturated Fatty Acid Prodrugs into Nanomedicines for Cancer Therapy. *Chemical Communications* 2018, 54:1996–1999.

[17] Sarwar H, Khalid HM, Basher MK, Mia MNH, Rahman MT, Jalal UM: Smart Nanocarrier-Based Drug Delivery Systems for Cancer Therapy and Toxicity Studies: A Review. *Journal of Advanced Research* 2018, 15:1–18.

[18] Li G, Sun B, Li Y, Luo C, He Z, Sun J: Small-Molecule Prodrug Nanoassemblies: An Emerging Nanoplatform for Anticancer Drug Delivery. *Small* 2021, 17:e2101460.

[19] Yang Y, Zuo S, Zhang J, Liu T, Li X, Zhang H, et al.: Prodrug Nanoassemblies Bridged by Mono-/Di-/Tri-Sulfide Bonds: Exploration is for Going Further. *Nano Today* 2022, 44:101480.

[20] He Q, Chen J, Yan J, Cai S, Xiong H, Liu Y, et al.: Tumor Microenvironment Responsive Drug Delivery Systems. *Asian Journal of Pharmaceutical Sciences* 2019, 15:416–448.

[21] Zhang M, Qin X, Zhao Z, Du Q, Li Q, Jiang Y, et al.: A Self-Amplifying Nanodrug to Manipulate the Janus-Faced

Acta Materia Medica

Nature of Ferroptosis for Tumor Therapy. *Nanoscale Horizons* 2022, 7:198–210.

[22] Sun B, Luo C, Zhang X, Guo M, Sun M, Yu H, et al.: Probing the Impact of Sulfur/Selenium/Carbon Linkages on Prodrug Nanoassemblies for Cancer Therapy. *Nature Communications* 2019, 10:3211.

[23] Kumar R, Han J, Lim HJ, Ren WX, Lim JY, Kim JH, et al.: Mitochondrial Induced and Self-Monitored Intrinsic Apoptosis by Antitumor Theranostic Prodrug: In Vivo Imaging and Precise Cancer Treatment. *Journal of the American Chemical Society* 2014, 136: 17836–17843.

[24] Boyle ST, Johan MZ, Samuel MS: Tumour-Directed Microenvironment Remodelling at a Glance. *Journal of Cell Science* 2020, 133:jcs247783.

[25] Du J, Lane LA, Nie S: Stimuli-Responsive Nanoparticles for Targeting the Tumor Microenvironment. *Journal of Controlled Release* 2015, 219:205–214.

[26] Li C, Wang J, Wang Y, Gao H, Wei G, Huang Y, et al.: Recent progress in drug delivery. *Acta Pharmaceutica Sinica B* 2019, 9:1145–1162.

[27] Sun B, Luo C, Yu H, Zhang X, Chen Q, Yang W, et al.: Disulfide Bond-Driven Oxidation- and Reduction-Responsive Prodrug Nanoassemblies for Cancer Therapy. *Nano Letters* 2018, 18:3643–3650.

[28] Li G, Sun B, Zheng S, Xu L, Tao W, Zhao D, et al.: Zwitterion-Driven Shape Program of Prodrug Nanoassemblies with High Stability, High Tumor Accumulation, and High Antitumor Activity. *Advanced Healthcare Materials* 2021, 10:e2101407.